Nonlinear Dyn (2019) 95:369–380
https://doi.org/10.1007/s11071-018-4569-3

ORIGINAL PAPER

One-soliton shaping and two-soliton interaction in the fifth-order variable-coefficient nonlinear Schrödinger equation

Chunyu Yang · Wenjun Liu · Qin Zhou · Dumitru Mihalache · Boris A. Malomed

Received: 25 May 2018 / Accepted: 19 September 2018 / Published online: 28 September 2018

Abstract One- and two-soliton analytical solutions of a fifth-order nonlinear Schrödinger equation with variable coefficients are derived by means of the Hirota bilinear method in this paper. Various scenarios of one-soliton shaping and two-soliton interaction and reshaping are investigated, using the obtained exact solutions and adjusting parameters of the underlying model. We find that widths of two colliding solitons can change without changing their amplitudes. Furthermore, we produce a solution in which two originally bound solitons are separated and are then moving in opposite directions. We also show that two colliding solitons can fuse to form a spatiotemporal train, composed of equally separated identical pulses. Moreover, we display that the width and propagation direction of the spatiotemporal train can change simultaneously. Effects of corresponding parameters on the one-soliton shaping and two-soliton interaction are discussed. Results of this paper may be beneficial to the application of optical self-routing, switching and path control.

Keywords Soliton shaping · Soliton interaction · Soliton manipulation · Fifth-order variable-coefficient nonlinear Schrödinger equation

C. Yang · W. Liu (✉)
State Key Laboratory of Information Photonics and Optical Communications, and School of Science, Beijing University of Posts and Telecommunications, P. O. Box 122, Beijing 100876, China
e-mail: jungliu@bupt.edu.cn

Q. Zhou (✉)
School of Electronics and Information Engineering, Wuhan Donghu University, Wuhan 430212, People's Republic of China
e-mail: qinzhou@whu.edu.cn

D. Mihalache
Horia Hulubei National Institute for Physics and Nuclear Engineering, P.O. Box MG-6, Magurele, RO 077125, Romania

B. A. Malomed
Department of Physical Electronics, School of Electrical Engineering, Faculty of Engineering, Tel Aviv University, Tel Aviv 69978, Israel

1 Introduction

The past decades have witnessed a constant growth in the number of studies on the existence, stability, and robustness of solitons (or more properly solitary waves) and their applications in diverse areas, such as optical fibers, matter waves (Bose–Einstein condensates), and water waves [1–9]. Finding exact solutions to nonlinear partial differential equations (PDEs) describing the evolution of localized waveforms is a significant subject in nonlinear science [10–33]. Many nonlinear evolution equations that model the realistic physical problems are variable-coefficient nonlinear PDEs [34–43]. They describe a plethora of physical effects in fluid dynamics, condensed matter physics, plasma physics, optics and photonics (especially in nonlinear fiber optics [44–50]). Solitons propagating in optical fibers may be adequately described by variable-coefficient nonlinear Schrödinger (VCNLS) equations, see book [2] and Refs. [44,50]. To increase the transmission rate, ultrashort (picosecond or subpicosecond) pulses are often used as data carriers, for which the higher-order dispersion (HOD) cannot be ignored. Therefore, finding analytical families of soliton solutions of nonlinear PDEs that incorporate higher-order terms, especially finding exact solutions of higher-order variable-coefficient NLS-type equations, is of great importance from both theoretical and experimental point of view [51–54].

Recently, many works addressed soliton solutions for the higher-order VCNLS equations, using various methods, such as the Darboux transformation and Hirota bilinear method [55–59]. In particular, breather solutions for a higher-order VCNLS equation have been found by means of the Darboux transformation [60], producing the effect of HOD on the obtained solutions, and the analysis of a sixth-order VCNLS equation [61] has yielded one- and two-soliton solutions with the help of the Hirota bilinear method, showing that HOD significantly affects velocities and amplitudes of the solitons. Further, a method to realize the transition between nonautonomous breathers and the nonautonomous multi-peak solitons for a VCNLS equation with HOD has been proposed in [62]. Recently, first- and second-order rogue-wave solutions for a fourth-order VCNLS equation have been obtained in Ref. [63], and effects of group velocity dispersion (GVD) and fourth-order dispersion (FOD) on rogue waves have been revealed.

In this paper, we investigate the following fifth-order VCNLS equation [64]:

$$\begin{aligned} &iu_x+\beta(x)\left(\frac{1}{2}u_{tt}+u|u|^2\right)-i\alpha(x)\left(u_{ttt}+6|u|^2u_t\right)\\ &\quad+\gamma(x)\left(u_{tttt}+6u^*u_t^2+4u|u_t|^2\right.\\ &\quad\left.+8|u|^2u_{tt}+2u^2u_{tt}^*+6u|u|^4\right)\\ &\quad-i\delta(x)\left(u_{ttttt}+10|u|^2u_{ttt}+30|u|^4u_t+10uu_tu_{tt}^*\right.\\ &\quad\left.+10uu_t^*u_{tt}+20u^*u_tu_{tt}+10u_t^2u_t^*\right)=0, \qquad (1)\end{aligned}$$

which may be used as an integrable model to describe the propagation of ultrashort pulses in inhomogeneous optical fibers. Here $u(x,t)$ is a complex function representing the envelope of the optical pulse, x is the normalized transmission distance, and t is the retarded time, the asterisk standing for the complex conjugate. Physically, real parameters $\beta(x)$, $\alpha(x)$, $\gamma(x)$, and $\delta(x)$ represent GVD, third-order dispersion (TOD), FOD, and the fifth-order dispersion, respectively. Equation (1) with constant coefficients has been proved to be completely integrable by using the Lax pair and Darboux transformations [64]. However, possible integrability of Eq. (1) with x-dependent coefficients $\alpha(x)$, $\beta(x)$, $\gamma(x)$ and $\delta(x)$ has not been studied before. In the present work, analytical one- and two-soliton solutions to Eq. (1) are derived by means of the Hirota bilinear method for some particular choices of these coefficient functions, such as the one give by Eqs. (15) and (16). A comprehensive analysis of integrability conditions for the x-dependent coefficients of Eq. (1) should be a subject of a separate work.

Based on the obtained solutions, we present different scenarios of soliton interactions and reshaping, by adjusting parameters of the governing model. In particular, we will demonstrate a possibility to have pulse widths of two interacting solitons changing after the collision, without a change in their amplitudes. In addition, we demonstrate that the state of two interacting solitons can be changed, after a certain propagation distance, from a bound state to a pair of separating solitons with different amplitudes and widths. Also, an interesting effect revealed by the exact solutions is that a spatiotemporal pulse train can be compressed in the course of the propagation.

The rest of the paper is arranged as follows. The bilinear form and one- and two-soliton solutions of Eq. (1) are derived in Sect. 2 via the Hirota method. In Sect. 3, the use of the model's parameters for shaping one-soliton states and control of two-soliton interactions is illustrated graphically, using the obtained exact one- and two-soliton solutions. Finally, conclusions are formulated in Sect. 4.

2 Bilinear forms and solutions of Eq. (1)

In this section, bilinear forms and one- and two-soliton analytical solutions of Eq. (1) are given, using the Hirota bilinear method [65,66].

2.1 Bilinear forms

To transform Eq. (1) into the Hirota bilinear form, we introduce a dependent-variable transformation,

$$u(x,t)=\frac{g(x,t)}{f(x,t)},$$

where $g(x,t)$ is a complex differentiable function, while $f(x,t)$ is a real one. Then Eq. (1) can be transformed into

$$
\begin{aligned}
& i\frac{D_x g\cdot f}{f^2}+\beta(x)\left(\frac{D_t^2 g\cdot f}{2f^2}-\frac{g}{2f}\frac{D_t^2 f\cdot f}{f^2}+\frac{g}{f}\frac{|g|^2}{f^2}\right)\\
&-i\alpha(x)\left(\frac{D_t^3 g\cdot f}{f^2}-3\frac{D_t g\cdot f}{f^2}\times\frac{D_t^2 f\cdot f}{f^2}\right.\\
&\left.+6\frac{|g|^2}{f^2}\frac{D_t g\cdot f}{f^2}\right)\\
&+\gamma(x)\left[\frac{D_t^4 g\cdot f}{f^2}-\frac{g}{f}\frac{D_t^4 f\cdot f}{f^2}+6\frac{g}{f}\left(\frac{D_t^2 f\cdot f}{f^2}\right)^2\right.\\
&-6\frac{D_t^2 g\cdot f}{f^2}\frac{D_t^2 f\cdot f}{f^2}+6\frac{g^*}{f}\left(\frac{D_t g\cdot f}{f^2}\right)^2\\
&+4\frac{g}{f}\frac{D_t g\cdot f}{f^2}\frac{D_t g^*\cdot f}{f^2}\\
&+8\frac{|g|^2}{f^2}\left(\frac{D_t^2 g\cdot f}{f^2}-\frac{g}{f}\frac{D_t^2 f\cdot f}{f^2}\right)\\
&\left.+2\frac{g^2}{f^2}\left(\frac{D_t^2 g^*\cdot f}{f^2}-\frac{g^*}{f}\frac{D_t^2 f\cdot f}{f^2}\right)+6\frac{g}{f}\frac{|g|^4}{f^4}\right]\\
&-i\delta(x)\left[\frac{D_t^5 g\cdot f}{f^2}-10\frac{D_t^3 g\cdot f}{f^2}\frac{D_t^2 f\cdot f}{f^2}\right.\\
&-5\frac{D_t g\cdot f}{f^2}\frac{D_t^4 f\cdot f}{f^2}+30\frac{D_t g\cdot f}{f^2}\left(\frac{D_t^2 f\cdot f}{f^2}\right)^2\\
&+10\frac{|g|^2}{f^2}\left(\frac{D_t^3 g\cdot f}{f^2}-3\frac{D_t g\cdot f}{f^2}\frac{D_t^2 f\cdot f}{f^2}\right)\\
&+30\frac{|g|^4}{f^4}\frac{D_t g\cdot f}{f^2}+10\frac{g}{f}\frac{D_t g\cdot f}{f^2}\left(\frac{D_t^2 g^*\cdot f}{f^2}\right.\\
&\left.-\frac{g^*}{f}\frac{D_t^2 f\cdot f}{f^2}\right)+10\frac{g}{f}\frac{D_t g^*\cdot f}{f^2}\left(\frac{D_t^2 g\cdot f}{f^2}\right.\\
&\left.-\frac{g}{f}\frac{D_t^2 f\cdot f}{f^2}\right)+20\frac{g^*}{f}\frac{D_t g\cdot f}{f^2}\left(\frac{D_t^2 g\cdot f}{f^2}\right.\\
&\left.\left.-\frac{g}{f}\frac{D_t^2 f\cdot f}{f^2}\right)+10\left(\frac{D_t g\cdot f}{f^2}\right)^2\frac{D_t g^*\cdot f}{f^2}\right]=0,
\end{aligned}
\tag{2}
$$

where the Hitota bilinear operators D_x^m and D_x^n are defined by [65,66]

$$
D_x^m D_t^n g(x,t)\cdot f(x,t)=\left(\frac{\partial}{\partial x}-\frac{\partial}{\partial x'}\right)^m \times\left(\frac{\partial}{\partial t}-\frac{\partial}{\partial t'}\right)^n g(x,t)f(x',t')\bigg|_{x'=x,t'=t}. \tag{3}
$$

Setting $D_t^2 f\cdot f=2|g|^2$, and according to the properties of the Hirota bilinear D-operator:

$$
\frac{D_t^4 f\cdot f}{f^2}=\left(\frac{D_t^2 f\cdot f}{f^2}\right)_{tt}+3\left(\frac{D_t^2 f\cdot f}{f^2}\right)^2, \tag{4}
$$

Eq. (2) can be simplified as

$$
\begin{aligned}
&\frac{\left[iD_x+\frac{\beta(x)}{2}D_t^2-i\alpha(x)D_t^3+\gamma(x)D_t^4-i\delta(x)D_t^5\right]g\cdot f}{f^2}\\
&-\frac{3\gamma(x)g^*\left(D_t^2 g\cdot g\right)}{f^3}\\
&-i\frac{5\delta(x)g_t^*\left(D_t^2 g\cdot g\right)}{f^3}-i\frac{10\delta(x)g^*\left(D_t g\cdot g_{tt}\right)}{f^3}\\
&-i\frac{5\delta(x)g^*\left(D_t^2 g\cdot g\right)f_t}{f^4}=0.
\end{aligned}
\tag{5}
$$

Introducing two complex auxiliary functions $r=r(x,t)$ and $s=s(x,t)$, the bilinear relations for Eq. (1) can be derived as

$$D_t^2 f\cdot f=2|g|^2, \tag{6a}$$

$$D_t^2 g\cdot g=sf, \tag{6b}$$

$$2D_t g\cdot g_{tt}+sf_t=rf, \tag{6c}$$

$$
\begin{aligned}
&\left[iD_x+\frac{\beta(x)}{2}D_t^2-i\alpha(x)D_t^3+\gamma(x)D_t^4-i\delta(x)D_t^5\right]g\cdot f\\
&-3\gamma(x)g^*s-i5\delta(x)g_t^*s=i5\delta(x)g^*r,
\end{aligned}
\tag{6d}
$$

where the Hitota bilinear operators D_x^m and D_x^n are defined by [65,66]

$$
D_x^m D_t^n g(x,t)\cdot f(x,t)=\left(\frac{\partial}{\partial x}-\frac{\partial}{\partial x'}\right)^m \times\left(\frac{\partial}{\partial t}-\frac{\partial}{\partial t'}\right)^n g(x,t)f(x',t')\bigg|_{x'=x,t'=t}. \tag{7}
$$

Equation (6) can be solved by expanding functions $g(x,t)$, $f(x,t)$, $r(x,t)$, and $s(x,t)$ in powers of a formal small parameter ε:

$$g(x,t)=\varepsilon g_1(x,t)+\varepsilon^3 g_3(x,t)+\varepsilon^5 g_5(x,t)+\cdots, \tag{8a}$$

$$f(x,t)=1+\varepsilon^2 f_2(x,t)+\varepsilon^4 f_4(x,t)+\varepsilon^6 f_6(x,t)+\cdots, \tag{8b}$$

$$r(x,t)=r_0(x,t)+\varepsilon^2 r_2(x,t)+\varepsilon^4 r_4(x,t)+\varepsilon^6 r_6(x,t)+\cdots, \tag{8c}$$

$$s(x,t)=s_0(x,t)+\varepsilon^2 s_2(x,t)+\varepsilon^4 s_4(x,t)+\varepsilon^6 s_6(x,t)+\cdots, \tag{8d}$$

where $g_m(x,t)$ $(m=1,3,5,\ldots)$, $r_n(x,t)$, and $s_n(x,t)$ $(n=0,2,4,6,\ldots)$ are complex functions and $f_l(x,t)$ $(l=2,4,6,\ldots)$ are real ones.

2.2 One-soliton solutions

To obtain the one-soliton solution for Eq. (1), we assume $g(x,t)=\varepsilon g_1(x,t)$, $f(x,t)=1+\varepsilon^2 f_2(x,t)$, $r(x,t)=r_0(x,t)$, $s(x,t)=s_0(x,t)$. The expressions of $g_1(x,t)$ and $f_2(x,t)$ are assumed to be

$$g_1(x,t)=e^{\theta},\quad f_2(x,t)=\sigma(x)e^{\theta+\theta^*}. \tag{9}$$

Here $\theta=k(x)+wt+d$, where $k(x)$ is a complex function, and w and d are complex constants. Then, we substitute expression (9) into Eq. (6). After some calculations, the constraints on the parameters can be obtained as follows:

$$k(x)=\int\left[\frac{i}{2}w^2\beta(x)+w^3\alpha(x)+iw^4\gamma(x)+w^5\delta(x)\right]dx,$$
$$r_0(x,t)=s_0(x,t)=0,\quad \sigma(x)=\frac{1}{(w+w^*)^2}. \tag{10}$$

Without loss of generality, we set $\varepsilon=1$, and the analytic one-soliton solution for Eq. (1) can be written as

$$u(x,t)=\frac{g_1(x,t)}{1+f_2(x,t)}. \tag{11}$$

2.3 Two-soliton solution

To obtain the two-soliton solution of Eq. (1), we assume $g(x,t)=\varepsilon g_1(x,t)+\varepsilon^3 g_3(x,t)$, $f(x,t)=1+\varepsilon^2 f_2(x,t)+\varepsilon^4 f_4(x,t)$, $r(x,t)=r_0(x,t)+\varepsilon^2 r_2(x,t)$ and $s(x,t)=s_0(x,t)+\varepsilon^2 s_2(x,t)$, while the expressions for $g_1(x,t)$, $g_3(x,t)$, $f_2(x,t)$, and $f_4(x,t)$ are taken as

$$g_1(x,t)=e^{\theta_1}+e^{\theta_2},$$
$$g_3(x,t)=\rho_1(x)e^{\theta_1+\theta_2+\theta_1^*}+\rho_2(x)e^{\theta_1+\theta_2+\theta_2^*},$$
$$f_2(x,t)=\varphi_1(x)e^{\theta_1+\theta_1^*}+\varphi_2(x)e^{\theta_1+\theta_2^*}+\varphi_3(x)e^{\theta_2+\theta_1^*}+\varphi_4(x)e^{\theta_2+\theta_2^*},$$
$$f_4(x,t)=\psi(x)e^{\theta_1+\theta_2+\theta_1^*+\theta_2^*}. \tag{12}$$

Here $\theta_j(x,t)=k_j(x)+w_jt+d_j$ $(j=1,2)$, where $k_j(x)$ are complex functions, and w_j and d_j are complex constants. Then, we substitute expression (12) into Eq. (6). After some calculations, the expressions for the parameters can be obtained as follows:

$$k_1(x)=\int\left[\frac{i}{2}w_1^2\beta(x)+w_1^3\alpha(x)+iw_1^4\gamma(x)+w_1^5\delta(x)\right]dx,$$
$$k_2(x)=\int\left[\frac{i}{2}w_2^2\beta(x)+w_2^3\alpha(x)+iw_2^4\gamma(x)+w_2^5\delta(x)\right]dx,$$
$$r_0(x,t)=s_0(x,t)=0,\quad r_2(x,t)=\zeta(x)e^{\theta_1+\theta_2},$$
$$s_2(x,t)=\xi(x)e^{\theta_1+\theta_2},\quad \xi(x)=2(w_1-w_2)^2,$$
$$\zeta(x)=-2(w_1-w_2)^2(w_1+w_2),$$
$$\varphi_1(x)=\frac{1}{(w_1+w_1^*)^2},\quad \varphi_2(x)=\frac{1}{(w_1+w_2^*)^2},$$
$$\varphi_3(x)=\frac{1}{(w_2+w_1^*)^2},\quad \varphi_4(x)=\frac{1}{(w_2+w_2^*)^2},$$
$$\rho_1(x)=\frac{\varphi_1(x)\varphi_3(x)\xi(x)}{2},$$
$$\rho_2(x)=\frac{\varphi_2(x)\varphi_4(x)\xi(x)}{2},$$
$$\psi(x)=\frac{\varphi_1(x)\varphi_2(x)\varphi_3(x)\varphi_4(x)|\xi(x)|^2}{4}. \tag{13}$$

We set $\varepsilon=1$, and the analytic two-soliton solution for Eq. (1) can be written as

$$u(x,t)=\frac{g_1(x,t)+g_3(x,t)}{1+f_2(x,t)+f_4(x,t)}. \tag{14}$$

3 Discussion

In this section, we will consider the effect of relevant model parameters on shaping of one-soliton states and control of the two-soliton interaction, and subsequent reshaping of the solitons after the collision. The obtained results will be illustrated graphically by using both three-dimensional plots and two-dimensional contour plots of the corresponding waveforms.

To investigate the effect of HOD on the reshaping of the fundamental soliton, we fix the coefficients of GVD, FOD, and fifth-order dispersion and only vary the value of TOD to show the change of the shape of the soliton in the course of the propagation, as displayed in Figs. 1 and 2. When the variable (x-dependent) TOD is taken as

$$\alpha(x)=\tan(Cx), \tag{15}$$

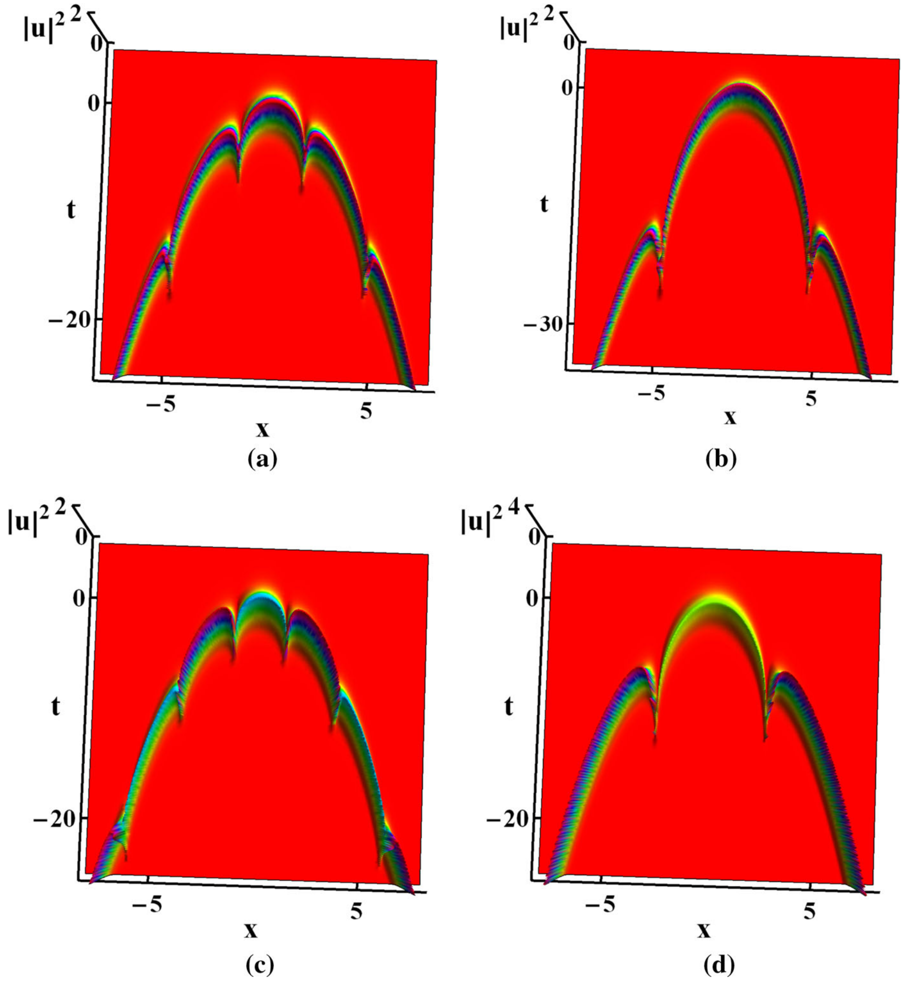

Fig. 1 One-soliton shaping based on the solution (11) with parameters: $w = 1$, $d = 2$, $\beta(x) = \gamma(x) = \delta(x) = x$. **a** $\alpha(x) = \tan(x)$; **b** $\alpha(x) = \tan(0.69x)$; **c** $\alpha(x) = \tan(1.3x)$; **d** $\alpha(x) = \tan(0.6x)$. In this figure and similar ones presented below, values of $|u|^2$ are shown by means of the vertical axis, which seems as a back-tilted left square bracket,[

with real constant C, and a linear function of x is chosen for coefficients of the inhomogeneous GVD, FOD, and fifth-order dispersion, i.e., we consider

$$\beta(x) = \gamma(x) = \delta(x) = x, \tag{16}$$

the reshaping of the fundamental soliton is shown in Fig. 1a for $C = 1$. It is clearly seen in Fig. 1a that the soliton trajectory in the (x, t) plane is a parabola-like one in this specific case. In the course of the soliton propagation, it shrinks to the narrowest state along the negative direction of t, and a phase flip occurs. Then, the width of the soliton expands, leading to the generation of left-right symmetric grooves in the course of the propagation. Further, the distance between two adjacent phase flips increases along the negative direction of t, while the amplitude of the soliton remains almost unchanged before and after the phase flip. If we adjust coefficient C in Eq. (15), the frequency of the soliton phase-flipping can be reduced without changing the soliton's amplitude, as shown in Fig. 1b. Furthermore, the amplitude of the soliton can be changed discontinuously by changing the same coefficient. As shown in Fig. 1c and d, the soliton's amplitudes, corresponding to the two sides of the phase flip, are quite different. These propagation scenarios show that both the width and amplitude of the soliton can be controlled by appropriately adjusting the HOD effects.

When we choose function $\tan(x)$ as the parameter of the fifth-order dispersion, and select the function $\sin(Cx)$ as the variable GVD, TOD, and FOD coefficients, the soliton performs periodic oscillations along x, as displayed in Fig. 2a, with its width changing periodically in the course of the propagation. C is a real

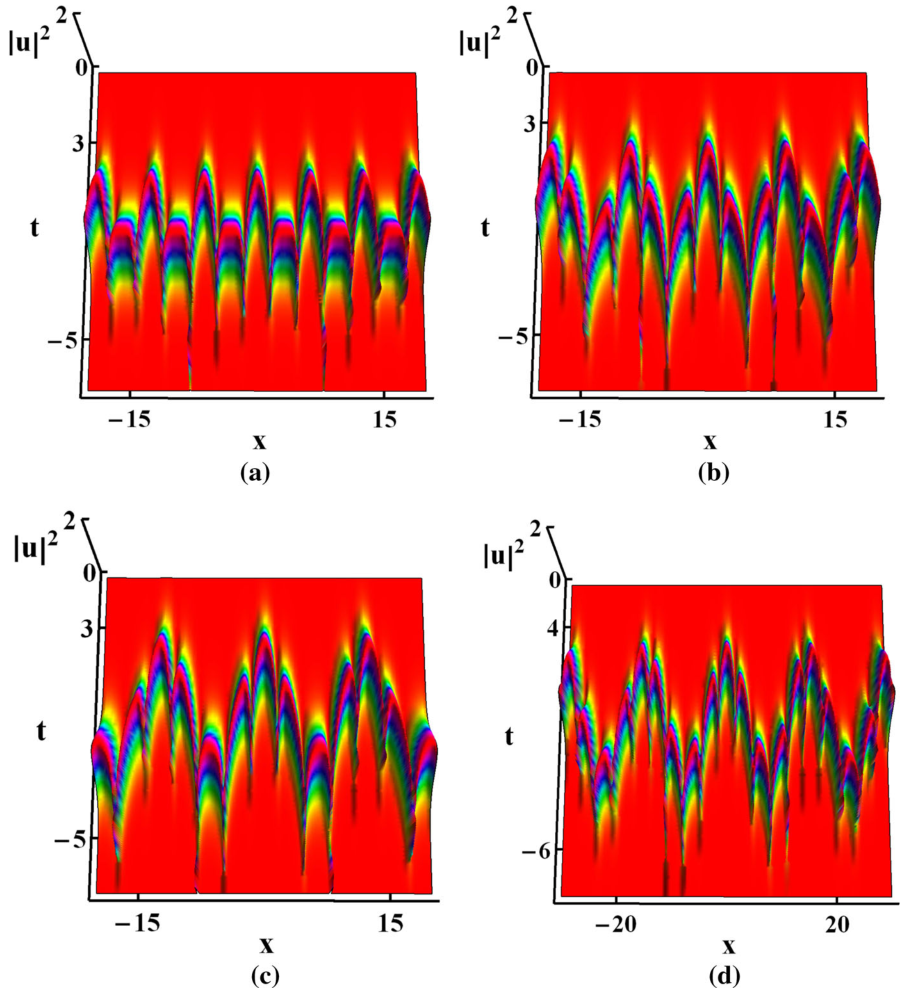

Fig. 2 One-soliton shaping based on the solution (11) with parameters: $w = 1$, $d = 2$, $\beta(x) = \sin(x)$, $\gamma(x) = \sin(x)$, $\delta(x) = \tan(x)$. **a** $\alpha(x) = \sin(x)$; **b** $\alpha(x) = \sin(0.69x)$; **c** $\alpha(x) = \sin(0.52x)$; **d** $\alpha(x) = \sin(0.42x)$

constant. In this case, we only vary the TOD coefficient, to observe its effect on the soliton transmission. As Fig. 2b–d shows, the periodic oscillations of the soliton can be controlled by adjusting coefficient C in $\sin(Cx)$ for the inhomogeneous TOD. It is also found that the variation of TOD affects the overall shape of the oscillations. Naturally, the oscillation intensity increases with the decrease of C.

In the above discussion of the reshaping of the fundamental soliton, we assumed that all HOD coefficients are functions of variable x. In contrast to that, in the analysis of two-soliton interactions, presented below, we assume that the GVD, TOD, and FOD coefficients are constant, while the fifth-order dispersion coefficient δ remains a function of x. As shown in Fig. 3a, widths of the two solitons change after the interaction, namely, one soliton expands while the other one gets compressed. Furthermore, amplitudes of the interacting solitons remain unchanged while their propagation directions in the (x, t) plane change after the collision. By appropriately modifying the values of complex constants w_1 and w_2, a noteworthy interaction scenario occurs, in which both solitons are compressed simultaneously after the collision, as shown in Fig. 3b. Besides that, we show that phases of the two solitons can be reversed when the values of $\beta(x)$, $\alpha(x)$, and $\gamma(x)$ are replaced by $-\beta(x)$, $-\alpha(x)$, and $-\gamma(x)$, as shown in Fig. 3c. These three generic scenarios of the two-soliton interaction are additionally illustrated by the corresponding contour plots in Fig. 4.

Figure 5 shows another interesting interaction effect, namely, that a complex of two interacting solitons can transform from a bound state to a state in which the solitons are well separated. The three panels in Fig. 5

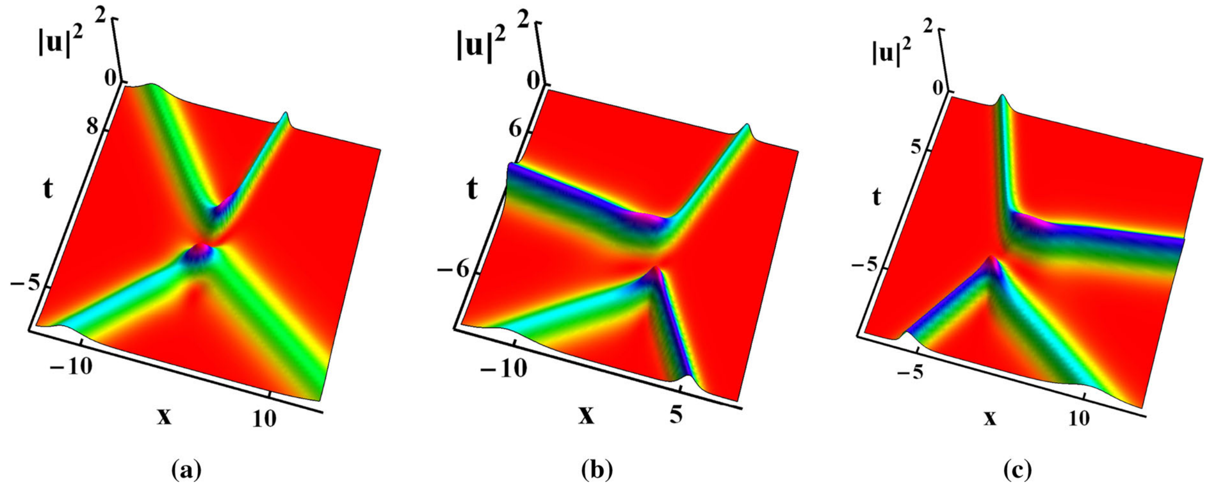

Fig. 3 The interaction of two solitons based on the solution (14) with parameters $d_1 = d_2 = 0$, $\beta(x) = \alpha(x) = \gamma(x) = 1$, $\delta(x) = \tanh(x)$. **a** $w_1 = 0.6 - 0.34i$, $w_2 = 0.72 + 0.72i$; **b** $w_1 = -0.88 + 0.016i$, $w_2 = -0.73 + 0.56i$; **c** The same as in (**b**), except for $\beta(x) = \alpha(x) = \gamma(x) = -1$

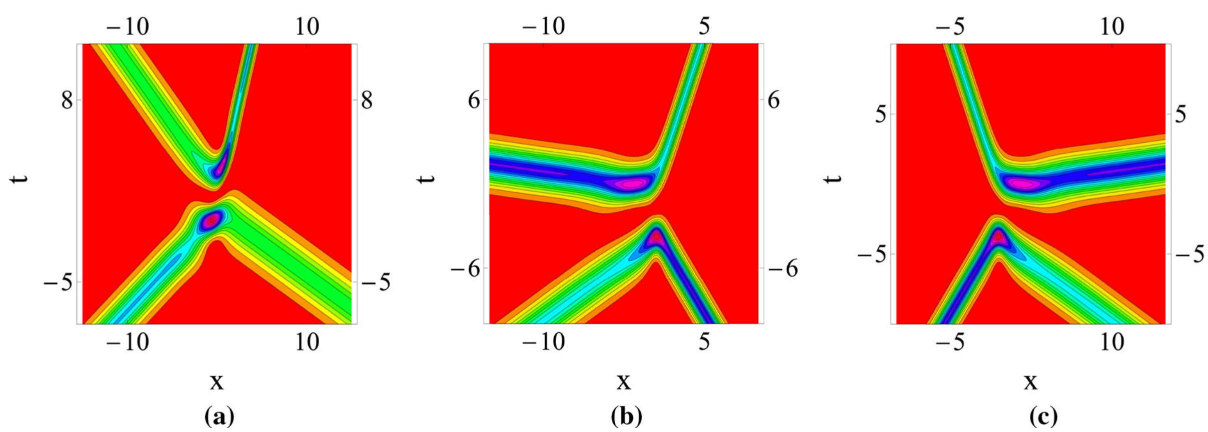

Fig. 4 Contour plots displayed in panels **a**, **b**, and **c** correspond to the three-dimensional plots in Fig. 3a, b, and c, respectively

show that the two solitons attract and repel each other periodically, generating a kind of a bound state. However, after propagating steadily for a certain distance, the solitons suddenly separate from each other and then propagate in different directions. These results may be used to design optical switches and to realize an optical path control. The interaction between two bound solitons and their subsequent separation are observed more clearly in Fig. 6, which shows contour plots corresponding to the interaction scenarios displayed in Fig. 5.

Apart from the bound-state soliton complex, another type of soliton–soliton interactions is displayed in Fig. 7. In Fig. 7a, fusion of two colliding solitons into a train of identical spatiotemporal pulses with equal separations between them is shown. The amplitudes of the emerging pulses are, obviously, much larger than the input amplitudes of the two colliding solitons. This effect may be used in specific applications in nonlinear fiber optics and high-power fiber lasers. Moreover, phases of two pulses can be flipped by replacing $\beta(x)$, $\alpha(x)$, and $\gamma(x)$ by $-\beta(x)$, $-\alpha(x)$, and $-\gamma(x)$, as shown in Fig. 7b. The formation of the spatiotemporal pulse train as the result of the collision can be observed more clearly in Fig. 8, which shows the corresponding contour plots.

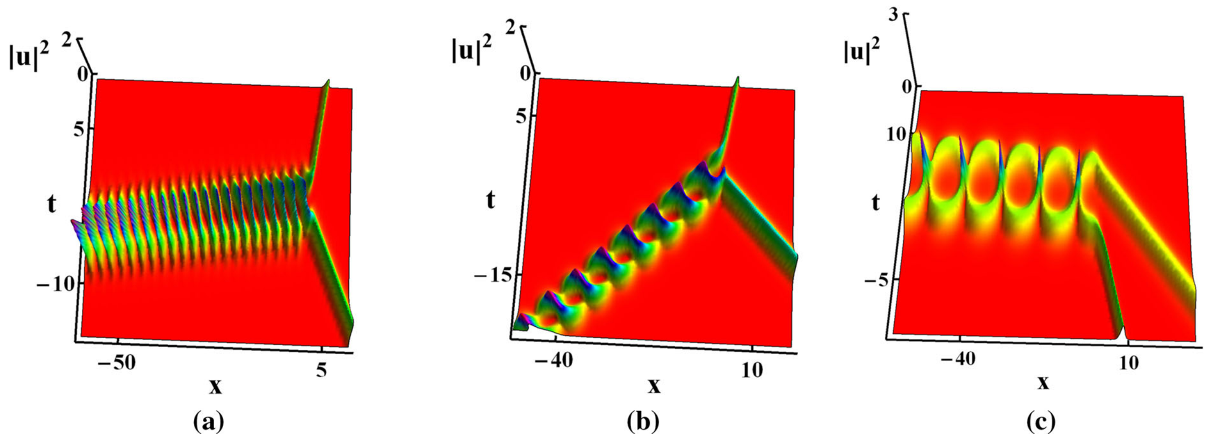

Fig. 5 The interaction of two solitons based on solution (14) with parameters $\delta(x) = \tanh(x)$, $d_1 = d_2 = 0$. **a** $\beta(x) = -0.56$, $\alpha(x) = 0.56$, $\gamma(x) = 0.31$, $w_1 = -0.75 - 0.8i$, $w_2 = -0.84 - 0.063i$; **b** The same as in (a), but with $\beta(x) = -1.75$, $\alpha(x) = 0.22$, $\gamma(x) = -0.095$; **c** The same as in (a), but $\beta(x) = 0.66$, $\alpha(x) = 1$, $\gamma(x) = 1$, $w_1 = 0.7 + 0.094i$, $w_2 = 0.91 + 0.031i$

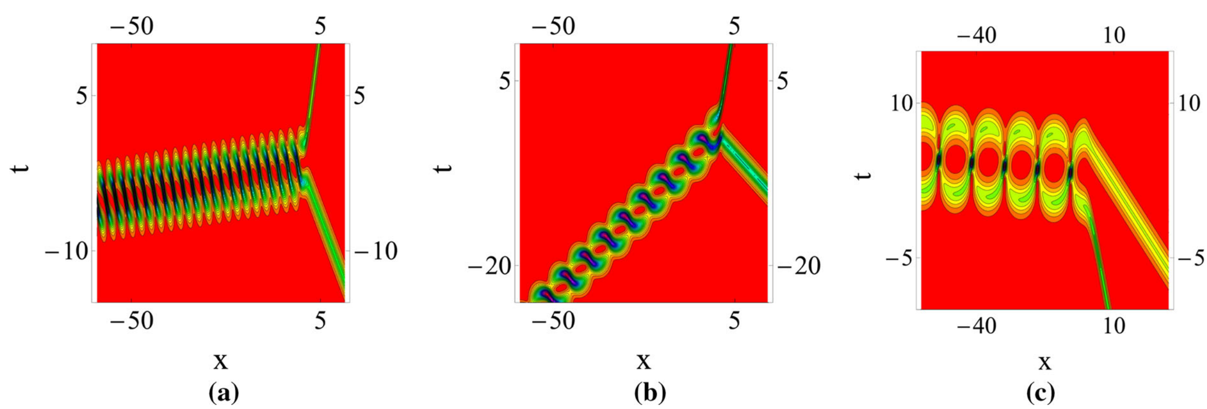

Fig. 6 Contour plots displayed in panels **a**, **b**, and **c** correspond to the three-dimensional plots in Fig. 5a, b, and c, respectively

Finally, Fig. 9 shows another noteworthy effect, in which the spatiotemporal pulse train compresses itself after propagating a certain distance. As shown in Fig. 9a, the spatiotemporal train propagates stably after performing the self-compression, maintaining identical shapes of the individual pulses and equal distances between them. However, the propagation direction of the compressed train changes in the (x, t) plane. We also note that, changing only the coefficients of dispersion terms in the underlying model one can adjust both the width of the spatiotemporal train and its propagation direction, keeping the self-compression property, as shown in Fig. 9b. In Fig. 10, contour plots additionally illustrate the dynamical scenarios from Fig. 9.

4 Conclusions

In this work, analytical one- and two-soliton solutions for the fifth-order nonlinear Schrödinger equation (1) with variable coefficients have been obtained by means of the Hirota bilinear method. Several generic scenarios of one-soliton shaping and two-soliton interaction and reshaping have been put forward based on exact one- and two-soliton solutions (11) and (14). According to the one-soliton solution (11), parabola-like and periodic oscillation patterns of the evolution of fundamental solitons have been presented in Figs. 1 and 2. The results show that both the amplitude and period of the soliton's oscillations can be controlled by changing the variable TOD coefficient $\alpha(x)$, which may help to

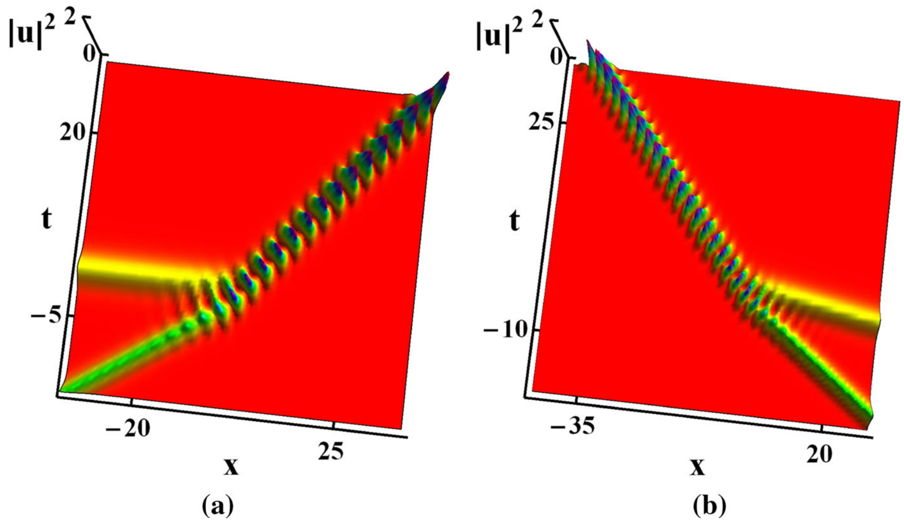

Fig. 7 The interaction of two solitons based on the solution (14) with parameters $\delta(x) = \tanh(x)$, $w_1 = 0.75 + 0.31i$, $w_2 = -0.56 - 0.61i$. **a** $\beta(x) = 0.92$, $\alpha(x) = 0.99$, $\gamma(x) = 1$; **b** $\beta(x) = -1.44$, $\alpha(x) = -1.51$, $\gamma(x) = -1.2$

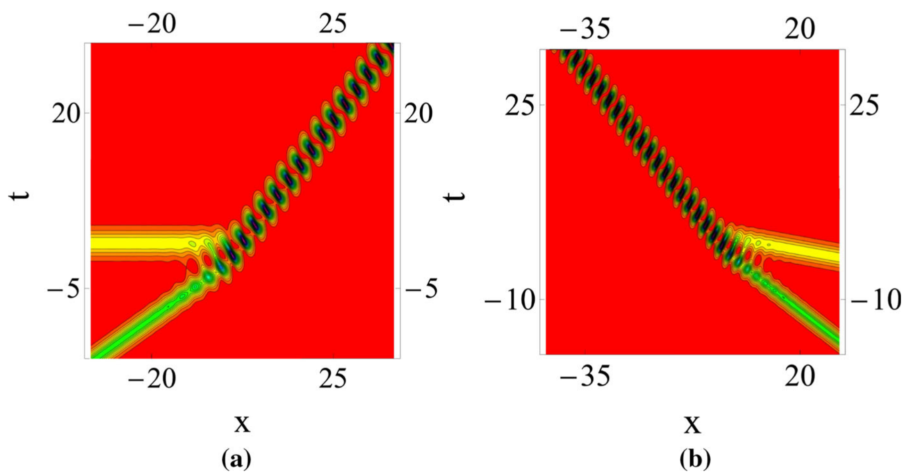

Fig. 8 Contour plots displayed in panels **a** and **b** correspond to the three-dimensional plots in Fig. 8a and b, respectively

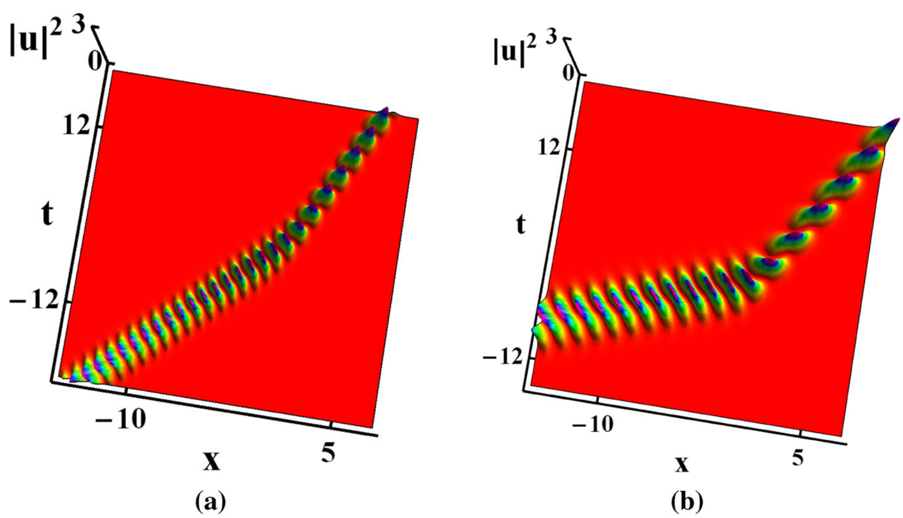

Fig. 9 The evolution of the soliton train based on solution (14) with parameters: $\delta(x) = \tanh(x)$, $d_1 = d_2 = 0$, $w_1 = 0.75 + 0.54i$, $w_2 = 0.73 - 0.855i$. **a** $\beta(x) = 1.8$, $\alpha(x) = 1.8$, $\gamma(x) = 1.79$; **b** $\beta(x) = \alpha(x) = \gamma(x) = 1$

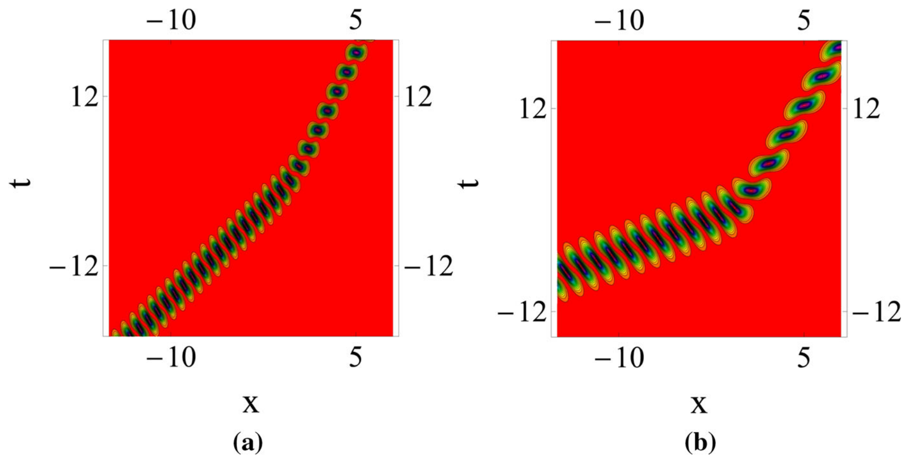

Fig. 10 Contour plots displayed in panels **a** and **b** correspond to the three-dimensional plots in Fig. 9a and b, respectively

apply dispersion management to solitons propagating in fibers with inhomogeneous higher-order dispersion. Using the two-soliton solution (14), we have found a scenario where one of the two interacting solitons widens, while the width of the other soliton is compressed, see Fig. 3a. For other sets of the model's parameters we have found that, after the interaction, the two solitons are compressed, see Fig. 3b. The analysis has also revealed an interesting effect, in which the complex composed of two interacting solitons can transform from a bound state into a pair of separating solitons, see Fig. 5. Further, in Fig. 7 we display the fusion of two colliding solitons into a train of identical spatiotemporal pulses with equal separations between them. In the latter case, the amplitude of the emerging train is much larger than amplitudes of the two input solitons. Also, a simple method to realize the soliton phase reversal has been proposed, see Figs. 3c, 4c, 7b, and 8b. Lastly, the exact solution demonstrates that the spatiotemporal pulse train can strongly compress itself, as shown in Figs. 9 and 10. The results reported in this work may be useful to the design of optical switches and path controllers, and for performing pulse compression in fiber laser systems.

Acknowledgements This work was supported by the National Natural Science Foundation of China (Grant Nos. 11875008 and 11674036), by the Beijing Youth Top-notch Talent Support Program (Grant No. 2017000026833ZK08), and by the Fund of State Key Laboratory of Information Photonics and Optical Communications (Beijing University of Posts and Telecommunications, Grant Nos. IPOC2016ZT04 and IPOC2017ZZ05). The work of Qin Zhou was supported by the National Natural Science Foundation of China (Grant Nos. 11705130 and 1157149), and this author was also sponsored by the Chutian Scholar Program of Hubei Government in China.

Compliance with ethical standards

Conflict of interest The authors declare that they have no conflict of interest.

References

1. Kivshar, Y.S., Agrawal, G.P.: Optical Solitons: From Fibers to Photonic Crystals. Academic Press, San Diego (2003)
2. Malomed, B.A.: Soliton Management in Periodic Systems. Springer, New York (2006)
3. Malomed, B.A., Mihalache, D., Wise, F., Torner, L.: Spatiotemporal optical solitons. J. Opt. B Quantum Semiclass. Opt. **7**, R53–R72 (2005)
4. Bagnato, V.S., Frantzeskakis, D.J., Kevrekidis, P.G., Malomed, B.A., Mihalache, D.: Bose–Einstein condensation: twenty years after. Rom. Rep. Phys. **67**, 5–50 (2015)
5. Malomed, B.A., Torner, L., Wise, F., Mihalache, D.: On multidimensional solitons and their legacy in contemporary atomic, molecular and optical physics. J. Phys. B **49**, 170502 (2016)
6. Malomed, B.A.: Multidimensional solitons: well-established results and novel findings. Eur. Phys. J. Spec. Top. **225**, 2507–2532 (2016)
7. Kevrekidis, P.G., Frantzeskakis, D.J.: Solitons in coupled nonlinear Schrödinger models: a survey of recent developments. Rev. Phys. **1**, 140–153 (2016)
8. Mihalache, D.: Multidimensional localized structures in optical and matter-wave media: a topical survey of recent literature. Rom. Rep. Phys. **69**, 403 (2017)
9. Chen, S., Baronio, F., Soto-Crespo, J.M., Grelu, P., Mihalache, D.: Versatile rogue waves in scalar, vector, and multidimensional nonlinear systems. J. Phys. A **50**, 463001 (2017)
10. Cao, Y.L., He, J.S., Mihalache, D.: Families of exact solutions of a new extended (2 + 1)-dimensional Boussinesq equation. Nonlinear Dyn. **91**, 2593–2605 (2018)

11. Liu, Y.B., Mihalache, D., He, J.S.: Families of rational solutions of the y-nonlocal Davey–Stewartson II equation. Nonlinear Dyn. **90**, 2445–2455 (2017)
12. Xing, Q.X., Wu, Z.W., Mihalache, D., He, J.S.: Smooth positon solutions of the focusing modified Korteweg-de Vries equation. Nonlinear Dyn. **89**, 2299–2310 (2017)
13. Liu, Y.B., Fokas, A.S., Mihalache, D., He, J.S.: Parallel line rogue waves of the third-type Davey–Stewartson equation. Rom. Rep. Phys. **68**, 1425–1446 (2016)
14. Yuan, F., Rao, J.G., Porsezian, K., Mihalache, D., He, J.S.: Various exact rational solutions of the two-dimensional Maccari's system. Rom. J. Phys. **61**, 378–399 (2016)
15. Chakraborty, S., Nandy, S., Barthakur, A.: Bilinearization of the generalized coupled nonlinear Schödinger equation with variable coefficients and gain and dark–bright pair soliton solutions. Phys. Rev. E **91**, 023210 (2015)
16. Loomba, S., Pal, R., Kumar, C.N.: Bright solitons of the nonautonomous cubic-quintic nonlinear Schödinger equation with sign-reversal nonlinearity. Phys. Rev. A **92**, 033811 (2015)
17. Wong, P., Liu, W.J., Huang, L.G., Li, Y.Q., Pan, N., Lei, M.: Higher-order-effects management of soliton interactions in the Hirota equation. Phys. Rev. E **91**, 033201 (2015)
18. Wazwaz, A.M., El-Tantawy, S.A.: A new integrable (3 + 1)-dimensional KdV-like model with its multiple-soliton solutions. Nonlinear Dyn. **83**, 1529–1534 (2016)
19. Chan, H.N., Malomed, B.A., Chow, K.W., Ding, E.: Rogue waves for a system of coupled derivative nonlinear Schödinger equations. Phys. Rev. E **93**, 012217 (2016)
20. Mirzazadeh, M., Arnous, A.H., Mahmood, M.F., Zerrad, E., Biswas, A.: Soliton solutions to resonant nonlinear Schödinger's equation with time-dependent coefficients by trial solution approach. Nonlinear Dyn. **81**(1–2), 277–282 (2015)
21. Ankiewicz, A., Kedziora, D.J., Chowdury, A., Bandelow, U., Akhmediev, N.: Infinite hierarchy of nonlinear Schödinger equations and their solutions. Phys. Rev. E **93**(1), 012206 (2016)
22. Kedziora, D.J., Ankiewicz, A., Chowdury, A., Akhmediev, N.: Integrable equations of the infinite nonlinear Schödinger equation hierarchy with time variable coefficients. Chaos **25**(10), 103114 (2015)
23. Ankiewicz, A., Soto-Crespo, J.M., Chowdhury, M.A., Akhmediev, N.: Rogue waves in optical fibers in presence of third-order dispersion, self-steepening, and self-frequency shift. JOSA B **30**(1), 87–94 (2013)
24. Ankiewicz, A., Akhmediev, N.: Rogue wave-type solutions of the mKdV equation and their relation to known NLSE rogue wave solutions. Nonlinear Dyn. **91**(3), 1931–1938 (2018)
25. Wazwaz, A.M.: Multiple-soliton solutions for a (3+1)-dimensional generalized KP equation. Commun. Nonlinear Sci. Numer. Simul. **17**(2), 491–495 (2012)
26. Mihalache, D.: Localized structures in nonlinear optical media: a selection of recent studies. Rom. Rep. Phys. **67**(4), 1383–1400 (2015)
27. Zhong, W., Belic, M.R., Huang, T.W.: Rogue wave solutions to the generalized nonlinear Schödinger equation with variable coefficients. Phys. Rev. E **87**, 065201 (2013)
28. Liu, W.J., Liu, M.L., OuYang, Y.Y., Hou, H.R., Ma, G.L., Lei, M., Wei, Z.Y.: Tungsten diselenide for mode-locked erbium-doped fiber lasers with short pulse duration. Nanotechnology **29**(17), 174002 (2018)
29. Dong, H.H., Zhao, K., Yang, H.W., Li, Y.Q.: Generalised (2 + 1)-dimensional super Mkdv hierarchy for integrable systems in soliton theory. E. Asian J. Appl. Math. **5**, 256 (2015)
30. Chen, J.C., Zhu, S.D.: Residual symmetries and soliton–cnoidal wave interaction solutions for the negative-order Korteweg-de Vries equation. Appl. Math. Lett. **73**, 136 (2017)
31. Zhang, X.E., Chen, Y., Zhang, Y.: Breather, lump and X soliton solutions to nonlocal KP equation. Comput. Math. Appl. **74**, 2341 (2017)
32. Zhao, H.Q., Ma, W.X.: Mixed lump–kink solutions to the KP equation. Comput. Math. Appl. **74**, 1399 (2017)
33. McAnally, M., Ma, W.X.: An integrable generalization of the D-Kaup–Newell soliton hierarchy and its bi-Hamiltonian reduced hierarchy. Appl. Math. Comput. **323**, 220 (2018)
34. Liu, W.J., Yang, C.Y., Liu, M.L., Yu, W.T., Zhang, Y.J., Lei, M.: Effect of high-order dispersion on three-soliton interactions for the variable-coefficients Hirota equation. Phys. Rev. E **96**(4), 042201 (2017)
35. Triki, H., Leblond, H., Mihalache, D.: Soliton solutions of nonlinear diffusion–reaction-type equations with time-dependent coefficients accounting for long-range diffusion. Nonlinear Dyn. **86**, 2115–2126 (2016)
36. Xie, X.Y., Tian, B., Chai, J., Wu, X.Y., Jiang, Y.: Dark soliton collisions for a fourth-order variable-coefficient nonlinear Schö dinger equation in an inhomogeneous Heisenberg ferromagnetic spin chain or alpha helical protein. Nonlinear Dyn. **86**(1), 131–135 (2016)
37. Liu, W.J., Tian, B., Lei, M.: Dromion-like structures in the variable coefficient nonlinear Schödinger equation. Appl. Math. Lett. **30**, 28–32 (2014)
38. Liu, W.J., Yang, C.Y., Liu, M.L., Yu, W.T., Zhang, Y.J., Lei, M., Wei, Z.Y.: Bidirectional all-optical switches based on highly nonlinear optical fibers. EPL **118**(3), 34004 (2017)
39. Li, M., Xu, T., Wang, L., Qi, F.H.: Nonautonomous solitons and interactions for a variable-coefficient resonant nonlinear Schödinger equation. Appl. Math. Lett. **60**, 8–13 (2016)
40. Chai, J., Tian, B., Xie, X.Y., Sun, Y.: Conservation laws, bilinear Bäcklund transformations and solitons for a nonautonomous nonlinear Schödinger equation with external potentials. Commun. Nonlinear Sci. Numer. Simul. **39**, 472–480 (2016)
41. Zuo, D.W., Gao, Y.T., Xue, L., Feng, Y.J.: Lax pair, rogue-wave and soliton solutions for a variable-coefficient generalized nonlinear Sch ödinger equation in an optical fiber, fluid or plasma. Opt. Quantum Electron. **48**(1), 76 (2016)
42. Dai, C.Q., Zhu, H.P.: Superposed Akhmediev breather of the (3 + 1)-dimensional generalized nonlinear Schödinger equation with external potentials. Ann. Phys. **341**, 142–152 (2014)
43. Wang, Y.F., Tian, B., Li, M., Wang, P., Wang, M.: Integrability and soliton-like solutions for the coupled higher-order nonlinear Schö dinger equations with variable coefficients in inhomogeneous optical fibers. Commun. Nonlinear Sci. Numer. Simul. **19**(6), 1783–1791 (2014)
44. Liu, W.J., Liu, M.L., Yin, J.D., Chen, H., Lu, W., Fang, S.B., Teng, H., Lei, M., Yan, P.G., Wei, Z.Y.: Tungsten dise-

lenide for all-fiber lasers with the chemical vapor deposition method. Nanoscale **10**, 7971–7977 (2018)
45. Li, W.Y., Ma, G.L., Yu, W.T., Zhang, Y.J., Liu, M.L., Yang, C.Y., Liu, W.J.: Soliton structures in the (1 + 1)-dimensional Ginzburg–Landau equation with a parity-time-symmetric potential in ultrafast optics. Chin. Phys. B **27**(3), 030504 (2018)
46. Osman, M.S., Wazwaz, A.M.: An efficient algorithm to construct multi-soliton rational solutions of the (2 + 1)-dimensional KdV equation with variable coefficients. Appl. Math. Comput. **321**, 282–289 (2018)
47. Wazwaz, A.M.: Two-mode fifth-order KdV equations: necessary conditions for multiple-soliton solutions to exist. Nonlinear Dyn. **87**(3), 1685–1691 (2017)
48. Liu, M.L., Liu, W.J., Pang, L.H., Teng, H., Fang, S.B., Wei, Z.Y.: Ultrashort pulse generation in mode-locked erbium-doped fiber lasers with tungsten disulfide saturable absorber. Opt. Commun. **406**, 72–75 (2018)
49. Wazwaz, A.M., El-Tantawy, S.A.: A new (3 + 1)-dimensional generalized Kadomtsev–Petviashvili equation. Nonlinear Dyn. **84**(2), 1107–1112 (2016)
50. Yang, C.Y., Li, W.Y., Yu, W.T., Liu, M.L., Zhang, Y.J., Ma, G.L., Lei, M., Liu, W.J.: Amplification, reshaping, fission and annihilation of optical solitons in dispersion-decreasing fiber. Nonlinear Dyn. **92**(2), 203–213 (2018)
51. Liu, M.L., Liu, W.J., Yan, P.G., Fang, S.B., Teng, H., Wei, Z.Y.: High-power $MoTe_2$-based passively Q-switched erbium-doped fiber laser. Chin. Opt. Lett. **16**(2), 020007 (2018)
52. Liu, W.J., Zhu, Y.N., Liu, M.L., Wen, B., Fang, S.B., Teng, H., Lei, M., Liu, L.M., Wei, Z.Y.: Optical properties and applications for MoS_2-Sb_2Te_3-MoS_2 heterostructure materials. Photonics Res. **6**(3), 220–227 (2018)
53. Wazwaz, A.M., El-Tantawy, S.A.: New (3 + 1)-dimensional equations of Burgers type and Sharma–Tasso–Olver type: multiple-soliton solutions. Nonlinear Dyn. **87**(4), 2457–2461 (2017)
54. Liu, W.J., Liu, M.L., Lei, M., Fang, S.B., Wei, Z.Y.: Titanium selenide saturable absorber mirror for passive Q-switched Er-doped fiber laser. IEEE J. Sel. Top. Quantam **24**(3), 0901005 (2018)
55. Dai, C.Q., Liu, J., Fan, Y., Yu, D.G.: Two-dimensional localized Peregrine solution and breather excited in a variable-coefficient nonlinear Schödinger equation with partial nonlocality. Nonlinear Dyn. **88**(2), 1373–1383 (2017)
56. Wang, L., Li, S., Qi, F.H.: Breather-to-soliton and rogue wave-to-soliton transitions in a resonant erbium-doped fiber system with higher-order effects. Nonlinear Dyn. **85**(1), 389–398 (2016)
57. Liu, W.J., Yu, W.T., Yang, C.Y., Liu, M.L., Zhang, Y.J., Lei, M.: Analytic solutions for the generalized complex Ginzburg–Landau equation in fiber lasers. Nonlinear Dyn. **89**(4), 2933–2939 (2017)
58. Yu, W.T., Yang, C.Y., Liu, M.L., Zhang, Y.J., Liu, W.J.: Interactions of solitons, dromion-like structures and butterfly-shaped pulses for variable coefficient nonlinear Schrödinger equation. Optik **159**, 21–30 (2018)
59. Yang, J.W., Gao, Y.T., Feng, Y.J., Su, C.Q.: Solitons and dromion-like structures in an inhomogeneous optical fiber. Nonlinear Dyn. **87**(2), 851–862 (2017)
60. Wang, L., Zhang, J.H., Liu, C., Li, M., Qi, F.H.: Breather transition dynamics, Peregrine combs and walls, and modulation instability in a variable-coefficient nonlinear Schödinger equation with higher-order effects. Phys. Rev. E **93**, 062217 (2016)
61. Su, J.J., Gao, Y.T., Jia, S.L.: Solitons for a generalized sixth-order variable-coefficient nonlinear Schödinger equation for the attosecond pulses in an optical fiber. Commun. Nonlinear Sci. Numer. Simul. **50**, 128–141 (2017)
62. Cai, L.Y., Wang, X., Wang, L., Li, M., Liu, Y., Shi, Y.Y.: Nonautonomous multi-peak solitons and modulation instability for a variable-coefficient nonlinear Schödinger equation with higher-order effects. Nonlinear Dyn. **90**(3), 2221–2230 (2017)
63. Du, Z., Tian, B., Chai, H.P., Sun, Y., Zhao, X.H.: Rogue waves for the coupled variable-coefficient fourth-order nonlinear Schödinger equations in an inhomogeneous optical fiber. Chaos Solitons Frac. **109**, 90–98 (2018)
64. Chowdury, A., Kedziora, D.J., Ankiewicz, A., Akhmediev, N.: Soliton solutions of an integrable nonlinear Schödinger equation with quintic terms. Phys. Rev. E **90**, 032922 (2014)
65. Hirota, R.: Exact envelope-soliton solutions of a nonlinear wave equation. J. Math. Phys. **14**(7), 805–809 (1973)
66. Hirota, R., Ohta, Y.: Hierarchies of coupled soliton equations. I. J. Phys. Soc. Japan **60**(3), 798–809 (1991)